THE JOURNAL OF PHYSICAL CHEMISTRY B

Article

pubs.acs.org/JPCB

Application of a Fluorescent *C*-Linked Phenolic Purine Adduct for Selective N7-Metalation of DNA

Alireza Omumi, Christopher K. McLaughlin, David Ben-Israel, and Richard A. Manderville*

Departments of Chemistry and Toxicology, University of Guelph, Guelph, Ontario, Canada N1G 2W1

ABSTRACT: The *C*-linked phenolic adduct, C8-(2″-hydroxyphenyl)-2′-deoxyguanosine (*o*-PhOHdG), has been employed to study the impact of N7-metalation of 2′-deoxyguanosine (dG) within duplex DNA. The phenolic group of *o*-PhOHdG assists selective metal ion coordination by the N7-site of the attached dG moiety, which is the most important metal binding site in duplex DNA. The biaryl nucleobase probe *o*-PhOHdG is highly fluorescent in water (Φ_{fl} = 0.44), and changes in its absorption and emission were used to determine apparent association constants (K_a) for binding to Cu(II), Ni(II), and Zn(II). The nucleoside was found to bind Cu(II) (log K_a = 4.59) and Ni(II) (log K_a = 3.65) effectively, but it showed relatively poor affinity for Zn(II) (log K_a = 2.55). The fluorescent nucleobase *o*-PhOHdG was incorporated into a pyrimidine-rich oligonucleotide substrate (ODN1) and a purine-rich (ODN2) substrate to monitor selective binding of Cu(II) through fluorescence quenching of the enol emission of *o*-PhOHdG within the DNA substrates. The pyrimidine-rich substrate ODN1 was found to possess greater affinity for Cu(II) than the free nucleobase, while the purine-rich substrate ODN2 exhibited diminished Cu(II) binding affinity. The impact of Cu(II) on duplex stability and structure was determined using UV melting temperature analysis and circular dichroism (CD) measurements. These studies highlight the *syn* preference for Cu(II)-bound *o*-PhOHdG within ODN1 duplexes and demonstrate competitive Cu(II) binding by other natural dG nucleobases within ODN2. The metal binding properties of *o*-PhOHdG are compared to the structurally similar 2-(2′-hydroxyphenyl)benzoxazole (HBO) derivatives and the nucleoside C8-(2-pyridyl)-dG (2PydG) that has also been used to control N7-metal coordination in DNA. Our results show certain advantages to the use of *o*-PhOHdG that stem from its highly fluorescent nature in aqueous media and provide additional tools for studying the effects of N7-metalation on the structure and stability of duplex DNA.

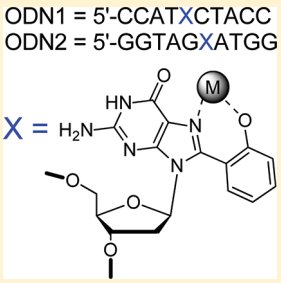

INTRODUCTION

The interaction of transition metal ions with DNA is an active field of research with applications in molecular biology, medicine, and material sciences.[1−3] A driving force for some of this research stems from the finding that DNA is the biological target of the antitumor drug cisplatin.[2] Coordination of bifunctional Pt(II) to two N7-sites of purine residues, especially guanine (G), in the major groove of duplex DNA, is thought to be critical for the therapeutic activity of the drug.[2] The coordination chemistry of DNA is now known to be dominated by examples of transition metal ions binding to the major groove N7-site of G.[4−12] Efforts have been made to understand the sequence preference of transition metal ion binding to N7 of G residues. NMR spectroscopy[7,10] combined with molecular modeling calculations[13] have suggested that transition metal ion coordination to N7 of G in duplex DNA is a highest occupied molecular orbital (HOMO)-controlled process. Experimental NMR evidence for metal ion binding typically relies on chemical shift data for the adjacent H8 of G that usually shifts downfield or undergoes line broadening upon N7 binding by transition metals.[7,10] However, H8 chemical shift data can be difficult to interpret due to conformational changes in duplex DNA upon metal ion binding, and furthermore, NMR lacks sensitivity for practical use in cellular environments.

Our research has recently focused on the structural properties of 2′-deoxyguanosine (dG) modified at the C8-site by phenolic residues.[14−21] Phenolic toxins can react at the C8-site of dG following metabolism into electrophilic radical species.[22−24] Phenoxyl radicals display ambident [oxygen (*O*) vs carbon (*C*)] reactivity toward dG to generate both *O*-linked and *C*-linked adducts.[25] The biaryl *C*-linked adducts are highly fluorescent, which makes them sensitive probes for gaining insight into their conformational preference within duplex DNA.[21] In this regard, the *ortho* (*o*)-*C*-linked adduct (*o*-PhOHdG (**1**), Figure 1) is structurally related to 2-(2′-hydroxyphenyl)benzoxazole (HBO) derivatives that have been used as fluorescent probes due to their ability to undergo an excited-state intramolecular proton transfer (ESIPT) process that is attractive for the design of emission indicators.[26−30] Thus, we previously reported on the ability of *o*-PhOHdG (**1**) to undergo ESIPT in nonprotic solvents to generate an emissive keto tautomer (Scheme 1)[14] and demonstrated how this trait can be used to predict the local solvent environment of **1** within duplex DNA.[21]

Due to the close proximity of the phenolic OH and the proton acceptor N atom within HBO systems, these molecules have also been used as metal-ion responsive fluorescent probes[28,31,32] and as metal chelating ligands for therapeutic applications.[33,34] Metal ion coordination inhibits ESIPT due to

Received: April 2, 2012
Revised: May 8, 2012
Published: May 18, 2012

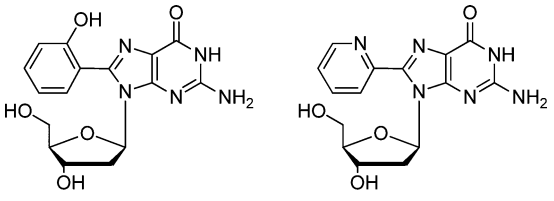

ODN1 = 5'-CCATXCTACC, X = dG, *o*-PhOHdG
ODN1'(N) = 5'-GGTAGNATGG, N = C, G, A, T
ODN2 = 5'-GGTAGXATGG, X = dG, *o*-PhOHdG
ODN2'(N) = 5'-CCATNCTCC, N = C, G, A, T

Figure 1. Structures of *ortho* (*o*)-PhOHdG (**1**), 2PydG (**2**), and oligonucleotide sequences.

Scheme 1

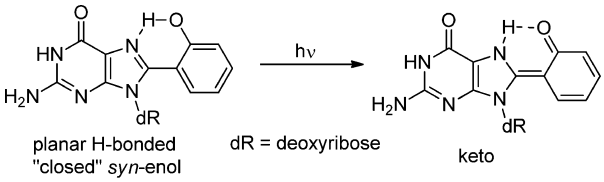

removal of the intramolecular hydrogen (H)-bond involving the phenolic OH group with the nearby N atom. Binding by paramagnetic metal ions quenches both the keto and enol emission of HBO systems, while closed-shell d^{10} metal ions, such as Zn(II), enhance the enol fluorescence emission intensity at the expense of keto emission, due to loss of the ESIPT process.[28,31,32]

For *o*-PhOHdG (**1**), the phenolic moiety would assist metal ion binding by N7 of dG, which is the most important metal binding site in duplex DNA.[1] Thus, fluorescent C8-substituted dG bases could provide a highly sensitive tool for detecting metal ion binding to specific N7-sites in DNA. During the course of our studies on metal binding by *o*-PhOHdG (**1**), Dumas and Luedtke reported[35] on the selective metal ion binding by the bidentate ligand C8-(2-pyridyl)-dG (2PydG (**2**), Figure 1) that coordinates transition metal ions by the N7 of dG and the 2-pyidyl N atom. This prompted us to report the selective binding of *o*-PhOHdG (**1**) to Cu(II), Ni(II), and Zn(II) as a comparison to the optical and metal binding properties of 2PydG (**2**) and the natural dG nucleobase. Our studies show certain advantages to the use of *o*-PhOHdG due to its highly fluorescent nature in aqueous media, which is important for sensing applications.

EXPERIMENTAL SECTION

Materials and Methods. Commercial compounds were used as received. 2-Hydroxyphenylboronic acid was purchased from Frontier Scientific (Logan, UT), $Pd(OAc)_2$ and 1,4-piperazinediethanesulfonic acid (PIPES) were from Sigma-Aldrich (Oakville, ON), and 3,3′,3″-phosphinidynetris-(benzenesulfonic acid) trisodium salt (TPPTS) was from Alfa Aesar (Ward Hill, MA). The synthesis of 8-bromo-2′-deoxyguanosine (8-Br-dG) and Suzuki cross-coupling of 2-hydroxyphenylboronic acid with 8-Br-dG to afford *o*-PhOHdG (**1**) were performed as described previously.[14,16] Oligonucleotide (ODN) substrates containing 8-Br-dG for the synthesis of ODN1 and ODN2 (Figure 1) were custom-made by Sigma Genosys (Canada) in 1 μmol scale using standard phosphoramidites and 8-Br-dG-CE phosphoramidite purchased from Glen Research (Sterling, VA). ^{1}H NMR spectra of o-PhOHdG (**1**) and 8-Br-dG were recorded in DMSO-d_6 at room temperature on a Bruker Avance 300 DPX and were referenced to DMSO-d_5H at 2.50 ppm. UV−vis and fluorescence emission spectra were recorded on a Cary 300-Bio UV−visible spectrophotometer and a Cary eclipse fluorescence spectrophotometer with built-in Peltier temperature controllers. Mass spectra were conducted at the Biological Mass Spectrometry Facility (BMSF) at the University of Guelph and were obtained from a Micromass/Waters Global Ultima quadrupole TOF using electrospray ionization. pH measurements were taken at room temperature with an Accumet 910 pH meter with an Accumet pH combination electrode with stirring. Any water used for buffers or spectroscopic solutions was obtained from a Milli-Q filtration system (18.2 MΩ).

Metal Binding Affinity of 1. The metal ion (M(II)) binding affinity of *o*-PhOHdG (**1**) was determined by UV−vis spectroscopy at 25 °C in 10 mM PIPES buffer, pH 7.2, containing 0.1 M NaCl. All M(II) solutions were prepared as stock solutions in water with the M(II) counterion being acetate. The stock solution of *o*-PhOHdG (**1**) (4.5 mM) was prepared in DMSO and diluted in 2.5 mL buffered water to a final concentration of 18 μM. An initial spectrum was taken ([M(II)] = 0), after which various metal equivalents were added to both the analytical and reference cuvettes. After each addition of M(II), the solution was stirred and allowed to equilibrate for 5 min, after which UV−vis spectra were measured from 400 to 250 nm. Double-reciprocal plots of $1/\Delta A$ (change in absorption) versus 1/[M(II)] afforded straight lines, from which the apparent association constant (K_a) was determined from K_a = (*y*-intercept)/(slope).[36]

Synthesis and Characterization of ODN1 and ODN2. The Suzuki−Miyaura coupling of 2-hydroxyphenylboronic acid with the brominated oligonucleotides (Br-DNA) (0.1 μmol) to afford ODN1 and ODN2 (Figure 1) was carried out as previously described.[21,37] Purification of the modified oligonucleotides was performed using an Agilent 1200 series HPLC equipped with an autosampler, autocollector, diode array detector, and fluorescence detector (excitation wavelength (λ_{ext}) = 290 nm; emission wavelength (λ_{em}) = 380 nm). Separations were carried out using a Phenomenox Clarity Oligo-RP C18 column, 50 × 4.60 mm^2, particle size 3 μm, using a gradient of 100% buffer A (95% 50 mM pH 7.2 triethylammonium acetate (TEAA)/5% acetonitrile) for the first 5 min to 20% buffer B (70% 50 mM TEAA/30% acetonitrile) over 30 min at a flow rate of 0.75 mL/min. The isolated yields of ODN1 and ODN2 were ∼80% based on UV quantification of the isolated product using ε_{260} (nearest neighbor method) for the unmodified oligonucleotides, 87,700 cm^{-1} M^{-1} for unmodified ODN1, and 106,000 cm^{-1} M^{-1} for unmodified ODN2 (i.e., X = G). Electrospray negative ionization (ESI$^-$) spectra of ODN1 and ODN2 were acquired as outlined previously.[37] ESI$^-$ MS ODN1 (*m*/*z*), calcd, 3039.6; observed $[M - 3H]^{3-}$ = 1012.2, found 3039.6; ODN2 (*m*/*z*), calcd, 3239.6; observed $[M - 4H]^{4-}$ = 808.9, found 3239.6.

Cu(II) Binding by ODN1 and ODN2. A stock $CuCl_2$ solution prepared in water was added in 5 μL increments to a standard 10 mm cuvette containing a solution of ODN1 or ODN2 at A_{260}/mL = 0.5 in 10 mM PIPES, pH 7.2, containing 200 mM NaCl. The λ_{em} at 390 nm (λ_{ext} = 290 nm) was monitored in the 305−550 nm region. The addition of $CuCl_2$ was continued until no further quenching of fluorescence at 390 nm for *o*-PhOHdG within the decanucleotides was

dx.doi.org/10.1021/jp303138s | J. Phys. Chem. B 2012, 116, 6158−6165

observed. The apparent association equilibrium constant K_a was determined from the ratio of the intercept and the slope from the double reciprocal plot of $F_o/(F_o - F)$ vs $1/[Cu]$.[36]

Thermal Melting Measurements. UV melting studies were carried out using methods outlined previously.[37] ODN1 or ODN2 (A_{260}/mL = 0.5) in the absence or presence of excess $CuCl_2$ (amount required to quench the emission of *o*-PhOHdG within the strands) was hybridized to its complementary strands of varying opposite base (N) in 10 mM PIPES, pH = 7.2 containing 200 mM NaCl. The change in absorbance at 260 nm was recorded for each duplex between 5 and 85 °C with a 0.5 °C/min gradient. The melting temperature (T_m) was determined by a first derivative calculation of the curve using the Cary 300 spectrophotometer Thermal software.

Circular Dichroism Measurements. Circular dichroism (CD) measurements were obtained on a Jasco J-815 CD spectropolarimeter equipped with a temperature controller. CD measurements were carried out at 5 and 35 °C in 10 mM PIPES, pH = 7.2 containing 200 mM NaCl with 0.5 A260/mL of ODN1 or ODN2 and their complementary strands (ODN1′ and ODN2′) in the absence and presence of $CuCl_2$. All CD spectra were measured from 400 to 200 at 0.5 nm increments with an averaging time of 1 s in a 0.1 cm path-length cuvette.

RESULTS

Photophysical and Metal Binding Properties of 1, 2, and dG. Photophysical parameters for *o*-PhOHdG (**1**),[14] 2PydG (**2**),[35] and dG[38] in H_2O and CH_3CN are listed in Table 1. In aqueous media, *o*-PhOHdG (**1**) shows a single absorption

Table 1. Photophysical Parameters for *o*-PhOHdG (1), 2PydG (2), and dG

adduct	λ_{max}, log ε, H_2O[c]	λ_{em}, Φ_{fl}, H_2O	brightness, H_2O[e]	λ_{max}, CH_3CN	λ_{em}, Φ_{fl}, CH_3CN
1	276, 4.25	395, 0.44	7824	281/318	383/481
2[a]	280/305, 4.30[d]	415, 0.02	400	316	395, 0.71
dG[b]	253, 4.14	334, 9.7×10^{-5}	1.33		

[a]Optical data for 2PydG (**2**) taken from ref 35. [b]Optical data for dG taken from ref 38. [c]Absorption and emission maxima in nanometers. [d]log ε for λ_{max} = 280 nm. [e]Brightness calculated as $\varepsilon_{\lambda max}\Phi_{fl}$.

at 276 nm and enol emission at 395 nm with a fluorescence quantum yield (Φ_{fl}) of 0.44. In CH_3CN, *o*-PhOH-dG (**1**) shows two absorption maxima at 281 and 318 nm, of almost equal intensity. Excitation at 281 nm gives rise to enol emission at 383 nm, while excitation at 318 nm gives rise to keto emission at 481 nm.[14] The absorbance at 318 nm was ascribed to a planar H-bonded "closed" *syn*-enol structure that undergoes ESIPT to generate the keto tautomer (Scheme 1). The absorbance at 281 nm that generates only enol emission was ascribed to a twisted ground state structure that lacks the intramolecular H-bond required for ESIPT.

In H_2O, 2PydG (**2**) shows two absorption maxima at 280 and 305 nm, with $\varepsilon_{280} \sim 20{,}000\ M^{-1}\ cm^{-1}$.[35] The probe exhibits quenched fluorescence in H_2O at 415 nm with $\Phi_{fl} \sim 0.02$. Protonation of the pyridyl nitrogen by bulk solvent upon photoexcitation is thought to cause nonemissive decay of **2** in H_2O.[35] As a result, *o*-PhOHdG (**1**) is ~20-fold brighter than 2PydG (**2**) in aqueous media. In CH_3CN, 2PydG (**2**) exhibits intense fluorescence emission at 395 nm with $\Phi_{fl} \sim 0.71$.[35] The solvent influence on the quantum yield of 2PydG (**2**) is attractive, as the probe possesses "turn-on" emissive characteristics when the nucleobase is shielded from an aqueous solvent environment.[39]

The metal binding affinity of *o*-PhOHdG (**1**) to Cu(II), Ni(II), and Zn(II) was monitored by UV−vis and fluorescence emission spectroscopy in aqueous buffer (10 mM PIPES buffer, pH 7.2, containing 0.1 M NaCl) at 25 °C (Figure 2). Binding of metal ions was initially monitored by UV−vis spectroscopy, which showed the appearance of a red-shifted broad absorbance with $\lambda_{max} \sim 340$ nm (Figure 2a−c). As discussed by Dumas and Luedtke,[35] the red-shifted absorbance is caused by binding of the positively charged metal ion to the C8-substituent, which enhances the donor−acceptor properties of the modified base, with the dG component acting as the donor and the metal-bound phenolic ring as the acceptor. The spectral changes upon addition of varying concentrations of metal ions allowed determination of apparent association constants (K_a). Double-reciprocal plots of the UV−vis binding data afforded straight lines, consistent with a 1:1 binding interaction.[36] Both Cu(II) and Ni(II) quenched the enol emission of *o*-PhOHdG (Figure 2d,e). In contrast, addition of Zn(II) caused a slight increase (~1.2-fold) in emission intensity with a shift in emission maxima from 395 nm for the free ligand to 420 nm (Figure 2f) for the Zn(II)-bound species, using an excitation wavelength of 330 nm. Similar metal ion binding titrations were also performed using the corresponding *para* (*p*-PhOHdG)[15,16,21] and *ortho* methoxy (*o*-PhOMedG)[14,17] adducts available in our laboratory. For these adducts, no UV−vis and fluorescence emission spectral changes accompanied addition of Cu(II), Ni(II), and Zn(II) (data not shown), highlighting the importance of the C2″−OH in *o*-PhOHdG (**1**) for metal ion binding.

Logarithms of apparent association constants (K_a) for metal ion binding by **1**, **2**,[35] and dG[8] are given in Table 2, which also includes negative logarithms of acidity constants for **1**[14,17] and dG.[9] The phenolic adduct **1** binds Cu(II) (log K_a = 4.59) and Ni(II) (logK_a = 3.65) effectively but shows relatively poor binding affinity to Zn(II) (log K_a = 2.55). Comparison of the Cu(II) and Ni(II) binding affinity of **1** to 2PydG (**2**) shows that **1** possesses greater affinity for Cu(II) than 2PydG (**2**) (~10-fold increase in K_a) but less affinity for Ni(II) (~3-fold decrease in K_a). For dG, two binding constants for Cu(II) and Ni(II) are given in Table 2. The log K_a values of 2.12 and 1.53 for Cu(II) and Ni(II) binding, respectively, represent stability constants for neutral dG binding to the metal ion.[8] For these transition metal ions, binding to N7 enhances the acidity of the N1H site and lowers the pK_a from 9.25 to ~6.7 ($\Delta pK_a \sim 2.5$) for Cu(II) binding and to ~7.6 ($\Delta pK_a \sim 1.7$) for Ni(II) binding.[8] Previously reported log K_a values of 4.7 and 3.2 represent stability constants for the anion of dG (deprotonated N1) binding to Cu(II) and Ni(II), respectively.[8] Both **1** and **2** bind Cu(II) and Ni(II) much more effectively than neutral dG (30- to ~400-fold increase in K_a). However, the anion of dG binds Cu(II) and Ni(II) with comparable affinity to that of the C8-substituted derivatives.

Cu(II) Binding by ODN1 and ODN2. To determine the metal binding properties of *o*-PhOHdG **1** within oligonucleotides, the pyrimidine-rich strand ODN1 (X = **1**) and the purine-rich strand ODN2 (X = **1**, Figure 1) were employed. These decanucleotide sequences were used previously to determine the structural impact of **1** and other C8−Ar-dG adducts on duplex stability.[21] Given that the free nucleoside **1** showed greatest affinity for Cu(II) (Table 2), our studies on

dx.doi.org/10.1021/jp303138s | J. Phys. Chem. B 2012, 116, 6158−6165

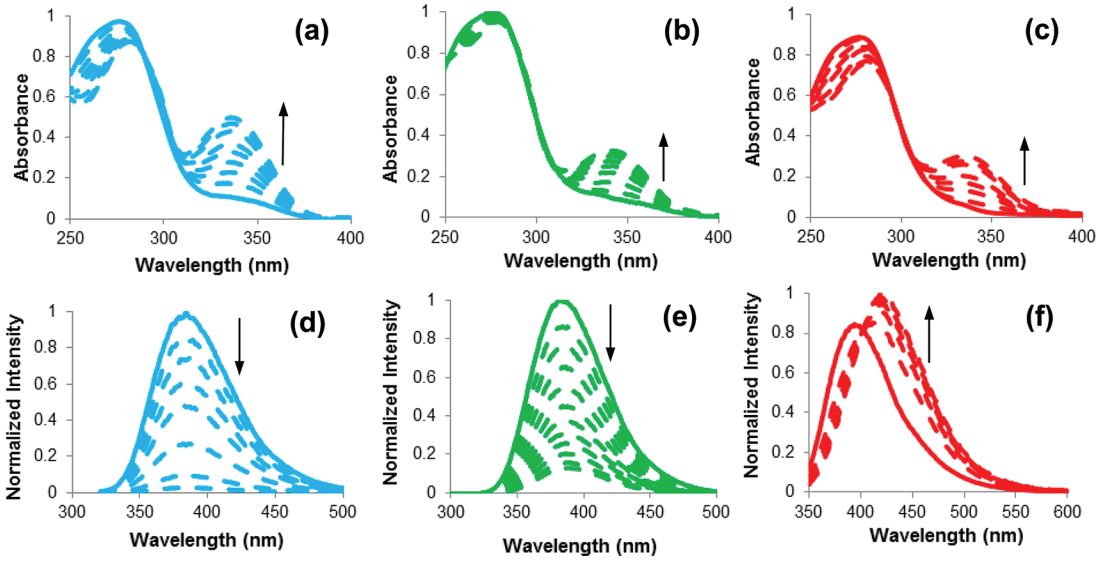

Figure 2. UV−vis absorbance of *o*-PhOHdG **1** as a function of added (a) Cu(II), (b) Ni(II), and (c) Zn(II) in 10 mM PIPES (pH 7.2, μ = 0.1 M NaCl) at 25 °C. Fluorescence emission of **1** as a function of added (d) Cu(II), (e) Ni(II), and (f) Zn(II) in 10 mM PIPES (pH 7.2, m = 0.1 M NaCl) at 25 °C, with excitation at 280 nm in parts d and e, and at 330 nm in part f.

Table 2. Thermodynamic Data for Metal Ion Binding by *o*-PhOHdG (1), 2PydG (2), and dG in Aqueous Solution

adduct	pK_a (N7H$^+$)	pK_a (N1H)	pK_a (PhOH)	log K_a Cu(II)	log K_a Ni(II)	log K_a Zn(II)
1	2.21 ± 0.17[c]	9.21 ± 0.03[d]	9.05 ± 0.02[e]	4.59 ± 0.04[f]	3.65 ± 0.02[f]	2.55 ± 0.03[f]
2[a]				3.59	4.12	
dG[b]	2.30 ± 0.04	9.24 ± 0.03		2.12/4.7	1.53/3.20	

[a]Metal binding data for 2PydG (**2**) taken from ref 35. [b]Metal binding and pK_a data for dG taken from ref 8. [c]Obtained from spectrophotometric titration at 20 °C (ref 17). [d]N1H pK_a value for *o*-MeOPhdG at 25 °C (ref 14). [e]Phenolic pK_a for N1-Me-*o*-PhOHdG at 25 °C (ref 14). [f]Determined from UV−vis titrations at 25 °C in 10 mM PIPES, pH 7.2, μ = 0.1 M NaCl.

the oligonucleotide substrates focused on Cu(II) binding. For these studies, a solution of $CuCl_2$ was added to the decanucleotide samples and fluorescence quenching of the enol emission of **1** was used as a criterion of metal binding. Metal ion complexation to *o*-PhOHdG (**1**) within the oligonucleotide substrates was also evident from the appearance of a new absorption peak with λ_{max} centered at ∼340 nm, as shown in Figure 3a for Cu(II) binding to ODN1. The inset to Figure 3a shows the decrease of florescence intensity for ODN1 (5 μM) upon addition of 10 μM $CuCl_2$ added in 0.5 equivalents (2.5 μM).

Figure 3b shows the fluorescence intensity for ODN1 and ODN2 (5 μM) as a function of Cu(II) concentration. For ODN1, the fluorescence intensity decreased in a linear fashion up to ∼11 μM Cu(II). In contrast, the fluorescence intensity of ODN2 showed very little decrease in intensity up to ∼11 μM Cu(II). This was then followed by a more drastic decrease in intensity up to ∼28 μM Cu(II). Apparent equilibrium constants (K_a) for Cu(II) binding by ODN1 and ODN2 were determined from double reciprocal plots of $F_o/(F_o - F)$ as a function of 1/[Cu], where F_o = initial fluorescence intensity and F = fluorescence upon addition of $CuCl_2$. Using the first five points for the Cu/ODN1 titration and the last five points for the Cu/ODN2 titration, straight lines were obtained, consistent with a 1:1 binding interaction. The association constant K_a was determined from the ratio of the intercept and slope, and it afforded a value of 8.3 × 10^4 M^{-1} (log K_a = 4.9 ± 0.16) for Cu(II) binding by ODN1 and a value of 1.1 × 10^4 M^{-1} (log K_a = 4.0 ± 0.2) for Cu(II) binding by ODN2. Thus, ODN1 has a greater affinity (∼ 2-fold increase in K_a) for Cu(II) than the

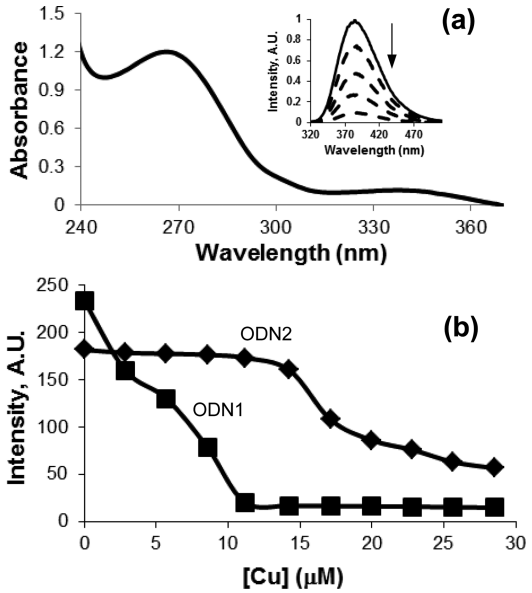

Figure 3. (a) UV−vis absorbance spectrum of Cu(II)-bound ODN1 (1.2 OD in 10 mM PIPES buffer, pH 7.2 containing 200 mM NaCl). Inset shows the decrease of florescence for ODN1 (5 μM) upon addition of 10 μM $CuCl_2$ added in 0.5 equivalents (2.5 μM). (b) Fluorescence emission (390 nm) intensity of ODN1 and ODN2 as a function of added Cu(II) in 10 mM PIPES (pH 7.2, μ = 0.2 M NaCl) at 25 °C, with excitation at 280 nm.

dx.doi.org/10.1021/jp303138s | J. Phys. Chem. B 2012, 116, 6158−6165

free nucleobase *o*-PhOHdG (**1**), while ODN2 does not bind Cu(II) as effectively as *o*-PhOHdG (~3.5-fold decrease in K_a). The decrease in Cu(II) binding by ODN2 (5′-GGTAG-XATGG) was ascribed to competitive binding by the other five natural dG nucleobases in the sequence. This competitive binding was observed in the early stages of the Cu(II)/ODN2 titration shown in Figure 3, where addition of Cu(II) failed to quench the fluorescence intensity of the modified base.

Effect of Cu(II) on Duplex Formation. To determine the impact of Cu(II) on duplex formation by ODN1 and ODN2, UV−vis thermal melting analysis (T_m) and CD experiments were carried out. The effect of Cu(II) on T_m for the decanucleotide duplexes was first determined for ODN1 (0.5 OD, ~5.7 μM), and the unmodified sequence (X = dG) was hybridized to 1 equiv of the complementary strand ODN1′(N), where N denotes the base opposite X (*o*-PhOHdG or dG, Figure 1). T_m values for the duplexes (Figure 4) were obtained

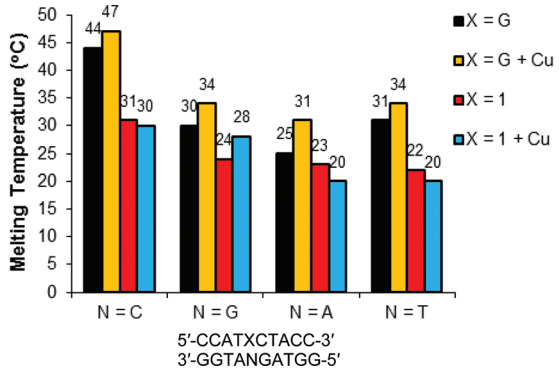

Figure 4. Melting temperatures of ODN1 (X = dG, **1**)/ODN1′(N) (5.7 μM strand) in the absence and presence of 20 μM $CuCl_2$ in 10 mM PIPES (pH 7.2, μ = 0.2 M NaCl).

either in the absence of Cu(II) or in the presence of 20 μM $CuCl_2$, prebound to ODN1 to ensure Cu(II) binding by *o*-PhOHdG within ODN1, as evidenced by fluorescence quenching (Figure 3b). In the absence of Cu(II), our previous studies have shown that *o*-PhOHdG decreases helix stability, especially when N = C within ODN1′, where ΔT_m = −13 °C compared to the control unmodified duplex.[21,37]

The T_m data shown in Figure 4 indicates that the presence of Cu(II) for the unmodified duplexes was a stabilizing influence, as evidenced by increased T_m values (ΔT_m = 3−6 °C). The stabilizing influence of Cu(II) may be due to nonspecific binding to the phosphate backbone. This interaction neutralizes negative charge and offsets electrostatic repulsion between the negatively charged single strands to favor duplex formation.[40] For the modified duplexes involving ODN1, only the X/G mismatch showed an increase in T_m upon Cu(II) binding (ΔT_m = 4 °C). The other modified duplexes showed a modest decrease in T_m (ΔT_m = −1−3 °C). The increase in duplex stability for the X/G mismatch in the presence of Cu(II) may stem from metal-mediated interactions between Cu-bound *o*-PhOHdG and the opposite dG to stabilize the helix.[3]

To investigate the possible impact of Cu(II) on duplex structure, CD measurements were performed at 5 °C on ODN1/ODN1′(N) duplexes in the presence or absence of $CuCl_2$ (20 μM). In the absence of Cu(II), the unmodified duplexes (X = dG) show characteristics of normal B-form DNA with approximately equal positive (275 nm) and negative (244 nm) bands with a crossover at 260 nm.[21,37] CD spectra for the unmodified duplexes in the presence of 20 μM Cu(II) (Figure 5) also showed characteristics for normal B-form DNA.

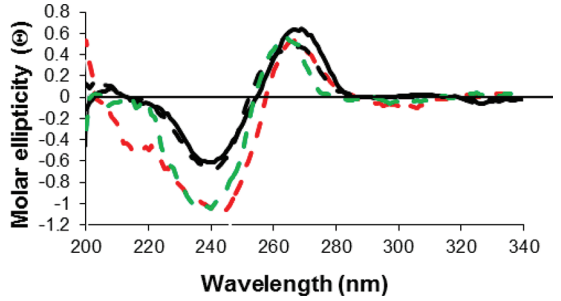

Figure 5. CD spectra of ODN1 (X = dG)/ODN1′(N) (0.5 A_{260}/mL of each strand) recorded at 5 °C in 20 μM $CuCl_2$, 10 mM PIPES (pH 7.2, μ = 0.2 M NaCl). N = C, solid black trace; N = T, dashed black trace; N = G, dashed green trace; N = A, dashed red trace.

Figure 6 shows the CD spectra for the Cu(II)-bound duplex of modified ODN1/ODN1′(C) at 5 °C (blue trace) and 35 °C

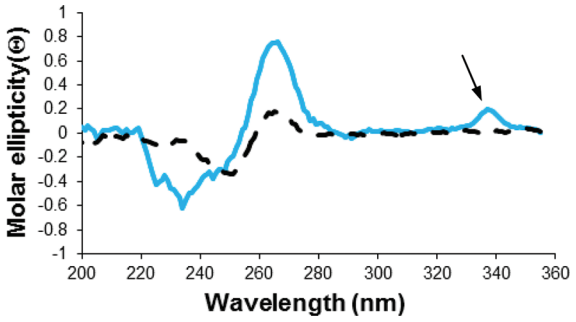

Figure 6. CD spectra of ODN1 (X = **1**)/ODN1′(C) (0.5 A_{260}/mL of each strand) in the presence of 20 μM $CuCl_2$, 10 mM PIPES (pH 7.2, *m* = 0.2 M NaCl). Solid blue trace, CD spectrum recorded at 5 °C, ICD signal at 340 nm indicated by the arrow. Dashed black trace, CD spectrum recorded at 35 °C.

(dashed black trace). The CD spectrum of Cu-ODN1/ODN1′(C) collected at 5 °C showed a clear positive induced CD (ICD) band at ~340 nm (indicated by the arrow in Figure 6), which corresponds to λ_{max} of the Cu(II)-bound *o*-PhOHdG adduct (Figures 2a and 3a). For related C8-dG adducts, ICD has been used as a useful marker for probing conformation,[41] and a positive ICD signal is indicative of a *syn*-adduct preference.[41] The observed ICD signal at 340 nm suggests that the Cu(II)-bound adduct is present in the *syn*-conformation, which places the metal complex within the chiral environment of the duplex. For the metal-free adduct, the utility of CD to define adduct conformation was limited by the fact that the absorption of *o*-PhOHdG overlaps with the absorption maxima of DNA.[21]

The CD spectrum recorded at 35 °C for Cu-ODN1/ODN1′(C) (dashed black trace, Figure 6) is above the T_m value for the duplex (Figure 4). The ICD signal at ~340 nm disappeared, and the intensity of the positive band at ~270 nm and the negative band ~240 nm decreased. These observations are consistent with removal of the Cu-bound adduct from the chiral environment and diminished π-stacking, as a result of duplex melting.

The interaction of Cu(II) with ODN2 differed significantly from the interactions outlined for ODN1. The purine-rich

dx.doi.org/10.1021/jp303138s | J. Phys. Chem. B 2012, 116, 6158−6165

ODN2 (X = **1**) required 80 μM $CuCl_2$ to completely quench the fluorescence of the modified base *o*-PhOHdG within the strand. Under these relatively high Cu(II) concentrations, typical sigmoidal thermal melting curves were not obtained from the samples containing modified and unmodified Cu(II)-ODN2 strands mixed with equal amounts of the complementary strands ODN2′(N). As a result, none of the samples formed stable duplexes under our experimental conditions and T_m values could not be determined. CD spectra for unmodified ODN2/ODN2′(N) in the presence of 80 μM $CuCl_2$ lacked a positive band at ∼270 nm and only showed a strong negative band at ∼245 nm (not shown), suggesting duplex denaturation through Cu(II)-binding to the nucleobases.[42]

DISCUSSION

As pointed out by Dumas and Luedtke,[35] C8-substituted purines provide new tools for measuring the impact of N7-metalation on the structure and electronic properties of nucleic acids. Attachment of an aryl ring to the C8-site of dG can generate fluorescent biaryl nucleobases that provide high sensitivity for probing structural dynamics and charge transfer in nucleic acids.[39,43,44] The addition of an *o*-substituent on the C8-aryl ring can assist metal ion binding by the N7-site of the dG moiety. This allows use of fluorescence spectroscopy to monitor selective metal ion binding at the N7-site of dG, which plays a critical role in transition metal ion binding by nucleic acids.[2,4−13]

To study selective N7-metalation of dG, we employed the nucleobase *o*-PhOH-dG (**1**), which contains an *o*-OH substituent on the C8-aryl ring and is structurally related to 2-(2′-hydroxyphenyl)benzoxazole (HBO) compounds that are used as metal-ion responsive fluorescent probes.[28,31,32] Initially, we determined the Cu(II), Ni(II), and Zn(II) binding affinity of the free nucleobase **1** in aqueous media (pH 7.2, Table 2). For a series of water-soluble 2-(2′-hydroxyphenyl)benzazole derivatives, Henary and Fahrni determined the Zn(II) binding affinities and found that the heteroatom in the benzazole ring system played a dramatic impact on Zn(II) binding,[28] as outlined in Scheme 2. The imidazole ligand (HBI) possessed

Scheme 2

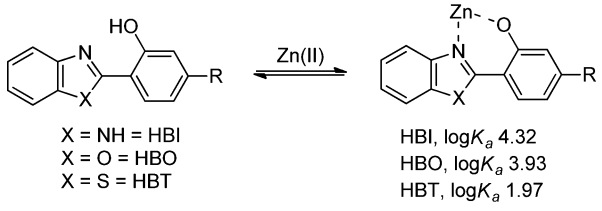

the highest affinity for Zn(II) (log K_a = 4.32), followed by HBO (log K_a = 3.93), while the thiazole ligand (HBT) exhibited a significantly lower affinity (log K_a = 1.97), which is more comparable to the Zn(II) binding affinity of the nucleobase **1** (log K_a = 2.55). Coordination of Zn(II) to the water-soluble benzazole derivatives was accompanied by deprotonation of the phenolic oxygen, which in addition to the benzazole nitrogen atom, acts as a donor atom in the Zn(II) complex.[28] Thus, the Zn(II) binding affinity of the benzazole derivatives will depend on the donor abilities of the benzazole nitrogen and phenolic oxygen atoms, together with the conformation of the ligand. In Scheme 2, the ligands are depicted in the *cis*-enol form, which is required for metal ion complexation and is the favored conformation in nonprotic solvents due to intramolecular H-bonding.[26−28] However, in protic solvents where the ligands are intermolecularly H-bonded with solvent, they can be susceptible to rotation to the *trans*-enol form with the phenolic OH group *cis* to the X atom.[45]

The water-soluble HBI analogue possesses a pK_a of 5.90 for deprotonation of the benzimidazole nitrogen and 8.63 for deprotonation of the phenolic OH group.[28] Henary and Fahrni were unable to determine pK_a values for the protonated HBO and HBT water-soluble analogues, but protonated HBO[46] and HBT[47] have pK_a values of ∼1.30, while the N7H$^+$ pK_a of **1** is ∼2.21 (Table 2). Thus, in terms of nitrogen atom donor capabilities, the nitrogen in HBI is a considerably better donor than the nitrogen atoms in the nucleobase **1** and the HBO and HBT ligands. This factor would account, in part, for the superior Zn(II) binding affinity of the HBI ligand versus **1**, HBO, and HBT. The phenolic pK_a values of the water-soluble derivatives were 9.28 for HBO and 8.25 for HBT,[28] while the phenolic pK_a of **1** is ∼9.21 (Table 2). Thus, in terms of phenolic oxygen atom donor capabilities, the order is HBO > **1** > HBI > HBT. Given that the nitrogen atom in **1** is a better donor than the corresponding nitrogen atoms in HBO and HBT, while the phenolic pK_a values for **1** and HBO do not significantly differ, factors other than donor atom abilities must play a role in Zn(II) binding by these ligands.

Previous studies on the structures of HBO and HBT ligands have demonstrated that in the HBT ligand the hydroxyphenyl group is much more susceptible to rotation than in the HBO ligand.[45] In polar protic solvents, the *trans*-enol form of HBT is much more stable that the *cis*-enol form that is required for Zn(II) binding. This is not the case for HBO, where the planar *cis*-enol form is the most stable structure. These differences in conformational preferences for HBO versus HBT[45] would be expected to play a role in Zn(II) binding affinity and could provide a rationale for the relatively poor Zn(II) binding affinity displayed by the water-soluble HBT analogue. Since the Zn(II) binding affinity of the nucleobase **1** was comparable to that of HBT, the conformation of **1** is also expected to play a role in its relatively weak Zn(II) binding affinity compared to that of the HBO analogue. Previous DFT calculations on the structure of **1** indicate that the hydroxyphenyl group is twisted by ∼25° versus the dG moiety in the lowest energy *syn* structure.[16−18] This degee of twist suggests that the hydroxyphenyl group in **1** is susceptible to rotation, as noted for the HBT analogue. Steric hindrance provided by the deoxyribose sugar moiety in **1** may also diminish the Zn(II) binding affinity relative to that of HBO, which is present in the favored *cis*-enol structure required for effective metal ion complexation.

The nucleobase **1** was found to bind Cu(II) (log K_a = 4.59) much more effectively than Zn(II), which is also typical for HBO analogues.[31,33] The nucleobase **1** also possesses greater affinity for Cu(II) than 2PydG (**2**) and neutral dG (Table 2). However, coordination of Cu(II) to the N7-site of dG is known to facilitate ionization of N1H, and a drop in its pK_a value, from ∼9.24 in free dG to ∼6.7 in Cu-dG, occurs.[8] Thus, at pH 7.2, dG will be converted into the anionic species upon Cu(II) binding and the anion of dG binds Cu(II) effectively (log K_a = 4.7). This suggests that dG may compete with **1** for Cu(II) binding within oligonucleotides, consistent with our data on Cu(II) binding by ODN2. Insertion of **1** into the pyrimidine-rich strand ODN1, which lacks other dG bases, showed that the modified base **1** had greater affinity for Cu(II) than the free

dx.doi.org/10.1021/jp303138s | J. Phys. Chem. B 2012, 116, 6158−6165

nucleoside *o*-PhOHdG (**1**). However, the modified base **1** within the purine-rich strand ODN2 did not bind Cu(II) as effectively as the free nucleoside **1**. This was ascribed to competitive binding by the other five natural dG nucleobases within ODN2.

Interestingly, the Cu-bound ODN2 did not generate stable duplex structures when mixed with its complementary strand ODN2′. Sigel and co-workers have discussed in detail the effect of N7-metalation on the H-bonding properties of the nucleobases.[48] N1-deprotonation of metal-bound G causes loss of Watson−Crick base pairing with C, which can inhibit duplex formation. It is also important to point out that in our experiments Cu(II) was added directly to the oligonucleotide single-strands ODN1 and ODN2, and then the impact of the metal ion on duplex formation was determined. In the work carried out by Dumas and Luedtke on Cu(II) binding by 2PydG (**2**),[35] the modified nucleobase was incorporated into two different positions within the G-rich oligonucleotide 5′-AGGGAGGGCXCTGGXAGGAGGG (where X = 2PydG) and the strand was then either folded into a G-quadruplex structure or mixed with the C-rich complementary strand, prior to addition of transition metal ions. Under these conditions, inhibition of duplex formation through metal ion addition was not observed. This observation is consistent with the understanding that nucleobase ionization is suppressed in double-stranded DNA because the N1H of G is involved in H-bonding.[48] If the G base is unable to undergo ionization, then binding of Cu(II) by neutral dG will not compete effectively with Cu(II) binding by the C8-substituted bases (Table 2).[8] Thus, the C8-substituted bases provide insight into the differing metal ion binding properties of single-strand vs duplex DNA substrates.

For the pyrimidine-rich strand ODN1, Cu(II) addition did not inhibit duplex formation. Our previous studies have suggested that the modified base *o*-PhOHdG (**1**) adopts a *syn*-conformation within ODN1 upon hybridization to its complementary strand.[21] This positions the phenolic ring in the minor groove of the duplex and causes a significant drop in duplex stability (Figure 4), as the *syn* base is not Watson−Crick paired with the opposing C. For the Cu(II)-bound duplex ODN1:1′(C), the ICD signal at ∼340 nm (Figure 6) indicated that Cu(II)-bound **1** within the duplex also adopts a *syn*-conformation. Binding of the positively charged Cu(II) to the modified base **1** within ODN1 had little impact on duplex stability compared to the impact of the unbound modified base (Figure 4). These results differ from the findings reported by Dumas and Luedtke on the impact of 2PydG (**2**) on duplex formation.[35] The free nucleobase **2** causes only a slight decrease in duplex stability (ΔT_m ∼ −3−6 °C), while Cu(II) binding had a slight stabilizing influence (ΔT_m ∼ +2 °C). These differences likely arise from the conformational preference of the C8-substituted bases. An *anti*-conformational preference of the nucleobase **2** will permit Watson−Crick H-bonding with the opposing C, leading to little loss of thermal stability. The absorption maximum of metal-bound 2PydG (**2**) occurs in the 325−375 nm region, and CD spectra of the Cu(II)-bound duplexes in the 220−350 nm region lacked ICD signals,[35] suggesting that the pyrimidyl moiety does not reside in the chiral environment of the DNA helix. This observation, coupled with the relatively small loss of thermal stability, suggests an *anti*-conformation preference for **2**, with the pyrimidyl moiety located in the major groove of the duplex. That *o*-PhOHdG prefers to adopt a *syn*-conformation in duplex DNA[21] expands the potential applications of C8-substituted purines for studying the impact on N7-metalation in nucleic acid substrates.

Current efforts in our laboratory are focused on the conversion of *o*-PhOHdG into a phosphoramidite suitable for solid-phase DNA synthesis to expand these current studies and monitor selective N7-metalation by *o*-PhOHdG in a wider range of oligonucleotides. Given the *syn* preference of *o*-PhOHdG, it should be possible to monitor the impact of the positively charged metal ion on π-stacking within a suitably designed DNA substrate. Other potential applications include the design of duplex structures bearing *o*-PhOHdG that in the presence of various metal ions act as chiral catalysts.

CONCLUSION

Biaryl C8-substituted purine nucleobases are fluorescent tools for studying selective N7-metalation of purine bases within nucleic acid substrates. One tool that can be used for this purpose is the nucleobase C8-(2-pyridyl)-dG (2PydG), which exhibits selective binding of metal ions through the N7-site of dG and the 2-pyridyl nitrogen of the C8-substituent. In this study we employed the *ortho*-substituted *C*-linked phenolic adduct, 8-(2″-hydroxyphenyl)-2′-dG (*o*-PhOHdG), as an alternative tool for monitoring selective Cu(II) binding by two decanucleotide substrates (ODN1 and ODN2). Our results provide a comparison between the utilities of 2PydG and *o*-PhOHdG. A main difference that has emerged from our studies is the conformational preference of these two C8-substituted nucleobases. Our studies show that o-PhOHdG adopts the *syn*-conformation within duplex DNA for both the metal-free and Cu-bound species. This places the phenolic ring system in the minor groove of DNA or within the π-stack of the helix. In contrast, 2PydG appears to favor the *anti*-conformation, which places the pyridyl moiety in the major groove of duplex DNA. Thus, these two C8-substituted nucleobases can be employed in a complementary fashion to explore the impact of N7-metalation from the different grooves of the helix.

AUTHOR INFORMATION

Corresponding Author

*Tel: 1-519-824-4120, Ext. 53963. Fax: 1-519-766-1499. E-mail: rmanderv@uoguelph.ca.

Notes

The authors declare no competing financial interest.

ACKNOWLEDGMENTS

Financial support for this work was provided by the Natural Sciences and Engineering Research Council of Canada (NSERC), the Canadian Foundation for Innovation (CFI), and the Ontario Innovation Trust Fund (OIT).

REFERENCES

(1) Lippert, B. *Coord. Chem. Rev.* **2000**, *200*, 487−516.
(2) Jamieson, E. R.; Lippard, S. J. *Chem. Rev.* **1999**, *99*, 2467−2498.
(3) Clever, G. H.; Shionoya, M. *Coord. Chem. Rev.* **2010**, *254*, 2391−2402.
(4) Kagawa, T. F.; Geierstanger, B. H.; Wang, A. H.-J.; Ho, P. S. *J. Biol. Chem.* **1991**, *266*, 20175−20184.
(5) Geierstanger, B. H.; Kagawa, T. F.; Chen, S.-L.; Quigley, G. J.; Ho, P. S. *J. Biol. Chem.* **1991**, *266*, 20185−20191.
(6) Gao, Y.-G.; Sriram, M.; Wang, A. H.-J. *Nucleic Acids Res.* **1993**, *21*, 4093−4101.

(7) Moldrheim, E.; Andersen, B.; Frøystein, N. A.; Sletten, E. *Inorg. Chim. Acta* **1998**, *273*, 41−46.
(8) Song, B.; Zhao, J.; Griesser, R.; Meiser, C.; Sigel, H.; Lippert, B. *Chem.—Eur. J.* **1999**, *5*, 2374−2387.
(9) Da Costa, C. P.; Sigel, H. *Inorg. Chem.* **2003**, *42*, 3475−3482.
(10) Vinje, J.; Parkinson, J. A.; Sadler, P. J.; Brown, T.; Sletten, E. *Chem.—Eur. J.* **2003**, *9*, 1620−1630.
(11) Wan, C.; Cui, M.; Song, F.; Liu, Z.; Liu, S. *J. Am. Soc. Mass Spectrom.* **2009**, *20*, 1281−1286.
(12) Sigel, R. K. O.; Sigel, H. *Acc. Chem. Res.* **2010**, *43*, 974−984.
(13) Saito, I.; Nakamura, T.; Nakatani, K. *J. Am. Chem. Soc.* **2000**, *122*, 3001−3006.
(14) McLaughlin, C. K.; Lantero, D. R.; Manderville, R. A. *J. Phys. Chem. A* **2006**, *110*, 6224−6230.
(15) Sun, K. M.; McLaughlin, C. K.; Lantero, D. R.; Manderville, R. A. *J. Am. Chem. Soc.* **2007**, *129*, 1894−1895.
(16) Millen, A. L.; McLaughlin, C. K.; Sun, K. M.; Manderville, R. A.; Wetmore, S. D. *J. Phys. Chem. A* **2008**, *112*, 3742−3753.
(17) Schlitt, K. M.; Sun, K. M.; Paugh, R. J.; Millen, A. L.; Navarro-Whyte, L.; Wetmore, S. D.; Manderville, R. A. *J. Org. Chem.* **2009**, *74*, 5793−5802.
(18) Millen, A. L.; Manderville, R. A.; Wetmore, S. D. *J. Phys. Chem. B* **2010**, *114*, 4373−4382.
(19) Millen, A. L.; Churchill, C. D. M.; Manderville, R. A.; Wetmore, S. D. *J. Phys. Chem. B* **2010**, *114*, 12995−13004.
(20) Millen, A. L.; Kamenz, B. L.; Leavens, F. M. V.; Manderville, R. A.; Wetmore, S. D. *J. Phys. Chem. B* **2011**, *115*, 12993−13002.
(21) Omumi, A.; Millen, A. L.; Wetmore, S. D.; Manderville, R. A. *Chem. Res. Toxicol.* **2011**, *24*, 1694−1709.
(22) Dai, J.; Wright, M. W.; Manderville, R. A. *J. Am. Chem. Soc.* **2003**, *125*, 3716−3717.
(23) Dai, J.; Wright, M. W.; Manderville, R. A. *Chem. Res. Toxicol.* **2003**, *16*, 817−821.
(24) Dai, J.; Sloat, A. L.; Wright, M. W.; Manderville, R. A. *Chem. Res. Toxicol.* **2005**, *18*, 771−779.
(25) Manderville, R. A. *Can. J. Chem.* **2005**, *83*, 1261−1267.
(26) Mosquera, M.; Penedo, J. C.; Rios Rodríguez, M. C.; Rodríguez-Prieto, F. *J. Phys. Chem.* **1996**, *100*, 5398−5407.
(27) Abou-Zied, O.; Jimenez, R.; Thompson, E. H. Z.; Millar, D. P.; Romesberg, F. E. *J. Phys. Chem. A* **2002**, *106*, 3665−3672.
(28) Henary, M. M.; Fahrni, C. J. *J. Phys. Chem. A* **2002**, *106*, 5210−5220.
(29) Ogawa, A. K.; Abou-Zied, O. K.; Tsui, V.; Jimenez, R.; Case, D. A.; Romesberg, F. E. *J. Am. Chem. Soc.* **2000**, *122*, 9917−9920.
(30) Dupradeau, F.-Y.; Case, D. A.; Yu, C.; Jimenez, R.; Romesberg, F. E. *J. Am. Chem. Soc.* **2005**, *127*, 15612−15617.
(31) Ohshima, A.; Momotake, A.; Arai, T. *Tetrahedron Lett.* **2004**, *45*, 9377−9381.
(32) Sumalekshmy, S.; Fahrni, C. J. *Chem. Mater.* **2011**, *23*, 483−500.
(33) Rodríguez- Rodríguez, C.; Sánchez de Groot, N.; Rimola, A.; Álvarez-Larena, Á.; Lloveras, V.; Vidal-Gancedo, J.; Ventura, S.; Vendrell, J.; Sodupe, M.; González-Duarte, P. *J. Am. Chem. Soc.* **2009**, *131*, 1436−1451.
(34) Mazzitelli, C. L.; Rodriguez, M.; Kerwin, S.; Brodbelt, J. S. *J. Am. Soc. Mass Spectrom.* **2008**, *19*, 209−218.
(35) Dumas, A.; Luedtke, N. W. *Chem.—Eur. J.* **2012**, *18*, 245−254.
(36) Conners, K. A. *Binding constants. The measurement of molecular complex stability*; John Wiley & Sons: New York, 1987; p 152.
(37) Omumi, A.; Beach, D. G.; Baker, M.; Gabryelski, W.; Manderville, R. A. *J. Am. Chem. Soc.* **2011**, *133*, 42−50.
(38) Onidas, D.; Markovitsi, D.; Marguet, S.; Sharonov, A.; Gustavsson, T. *J. Phys. Chem. B* **2002**, *106*, 11367−11374.
(39) Dumas, A.; Luedtke, N. W. *J. Am. Chem. Soc.* **2010**, *132*, 18004−18007.
(40) Karpel, R. L.; Bertelsen, A. H.; Fresco, J. R. *Biochemistry* **1980**, *19*, 504−512.
(41) Liang, F.; Meneni, S.; Cho, B. P. *Chem. Res. Toxicol.* **2006**, *19*, 1040−1043.
(42) Lippert, B. *J. Am. Chem. Soc.* **1981**, *103*, 5691−5697.
(43) Sinkeldam, R. W.; Greco, N. J.; Tor, Y. *Chem. Rev.* **2010**, *110*, 2579−2619.
(44) Wilson, J. N.; Kool, E. T. *Org. Biomol. Chem.* **2006**, *4*, 4265−4274.
(45) Nagaoka, S.; Itoh, A.; Mukai, K.; Nagashima, U. *J. Phys. Chem.* **1993**, *97*, 11385−11392.
(46) Mordziński, A.; Grabowska, A. *Chem. Phys. Lett.* **1982**, *90*, 122−127.
(47) Potter, C. A. S.; Brown, R. G. *Chem. Phys. Lett.* **1988**, *153*, 7−12.
(48) Sigel, H.; Song, B.; Oswald, G.; Lippert, B. *Chem.—Eur. J.* **1998**, *4*, 1053−1060.